Granular flow trapped on an incline: Dynamics of the sandpile

B. Bonnier, J.-F. Boudet, and H. Kellay
CPMOH, UMR CNRS 5798, Université Bordeaux 1, 351 cours de la Libération, 33405 Talence Cedex, France
(Received 4 June 2003; revised manuscript received 25 July 2003; published 15 December 2003)

Experimental results have been recently reported for the dynamics of two-dimensional sand fronts formed by the trapping of a flow running down an inclined plane. We explain the scaling law observed for the front profiles and give their analytic expression using a simple phenomonelogical model for interfacial shapes and interfacial flows of granular materials.

DOI: 10.1103/PhysRevE.68.061302 PACS number(s): 45.70.Ht, 45.70.Mg, 45.70.Qj

I. INTRODUCTION

In the study of granular materials [1], the flow of granular matters on inclined surfaces is of fundamental interest [2]. Many investigations have been devoted to the uniform regime [3,4] and more generally to the time evolution of the surface of a sandpile [5,6]. In this context, the understanding of the formation and evolution of sand fronts, within phenomenological models of sandpiles surfaces [6], brings forth some fundamental problems as discussed recently [7]. In the framework of propagating sand fronts, the results of a set of experiments allowing the study of self-similar advancing fronts have been recently reported [8]. In these experiments a jet of granular materials running down an inclined plane P ends up being trapped and then feeds a heap starting to grow upstream. The observed advancing sand fronts have curved self-similar shapes allowing a direct test of the validity and applicability of such models.

Our aim in this work is to give a phenomenological analysis of the experimental results of Ref. [8] which are recalled in Sec. II. First, we propose an explanation of the self-similarity property of the sand fronts as a consequence, through the mass and energy conservation laws, of the experimental conditions, independent of any specified model. This is done in Sec. III within the formalism proposed by Bouchaud, Cates, Ravi Prakash, and Edwards (BCRE) in Ref. [6] which recognizes two populations of grains, immobile and rolling with a conversion term that governs how mobile grains become static and vice versa, and maintains a continuum description of the dynamics of the sandpiles profiles. Taking into account the particularities of the experimental conditions, we do not however use the BCRE model as in the case of avalanches, since the self-similarity property allows a direct determination of all the physical quantities once the deposition term or conversion term is known. We thus propose an ansatz to describe this term and give in Sec. III the associated sandpile profiles. In Sec. IV we present the study of the dynamics of the rolling species. The differences arising between the standard BCRE model and the present case are discussed in Sec. V with our conclusion.

II. SUMMARY OF EXPERIMENTAL RESULTS

The experiments we wish to consider for this theoretical analysis have been presented recently by Boudet *et al.* [8]. In these experiments (see Fig. 1), sand running down an inclined plane P (sandwiched between two transparent flat plates so that the geometry is quasi-two-dimensional) comes to a halt at a certain distance $L(\theta)$ from the injection point due to friction against the flat plane. Once the sand comes to a stop, a small pile is constructed by the incoming flux of sand and a front of static sand starts to climb up the slope. The quasi-two-dimensional sand fronts obtained experimentally are self-similar in time as shown in Fig. 2. Here several profiles of the dynamic fronts climbing up the inclined plane are shown at different instants of time. As the front moves upstream, its base length and its height grow in time. This growth is self-similar as shown in the upper left inset of this figure. All the profiles from the different instants of time can be collapsed onto a single curve once the two axes have been divided by the base length $X(t)$. The shape of these sand fronts is characterized by a linear tail with a time independent angle ϕ_0 with the inclined plane and a curved front whose initial tangent $T_1=\tan\phi_1$ is also constant in time. A consequence of the collapse of the different profiles is that the base length $X(t)$ grows as $t^{1/2}$ as illustrated in the upper right inset of Fig. 2.

The self-similarity of the sand fronts appears to be possible when the inclination angle θ of P with the horizontal is varied in the range $8°\leqslant\theta\leqslant\theta_l$, θ_l being the maximal inclination allowing trapping. The results of these experiments can be summarized as follows, where the dynamics are described in the orthogonal frame (OX,OZ) whose OX axis is along P with upstream orientation, the trapping event corresponding to the values $x=z=t=0$ (see Fig. 1). As mentioned above the base length of the sandpile $[0\leqslant x\leqslant X(t), z=0]$ increases as $X(t)\approx\sqrt{t}$ and its upper profiles

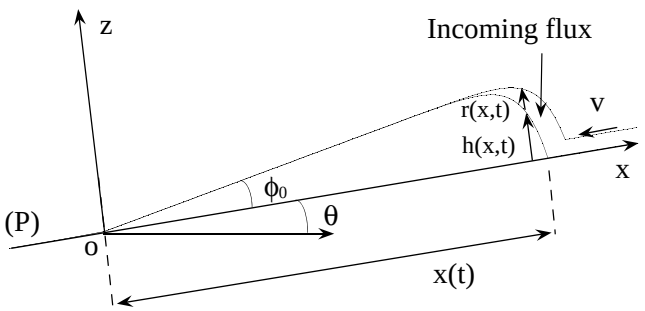

FIG. 1. Schematic of the sand fronts: An incoming flux of sand with velocity v down an inclined plane P gets trapped far downstream and a sand front starts to grow upstream.

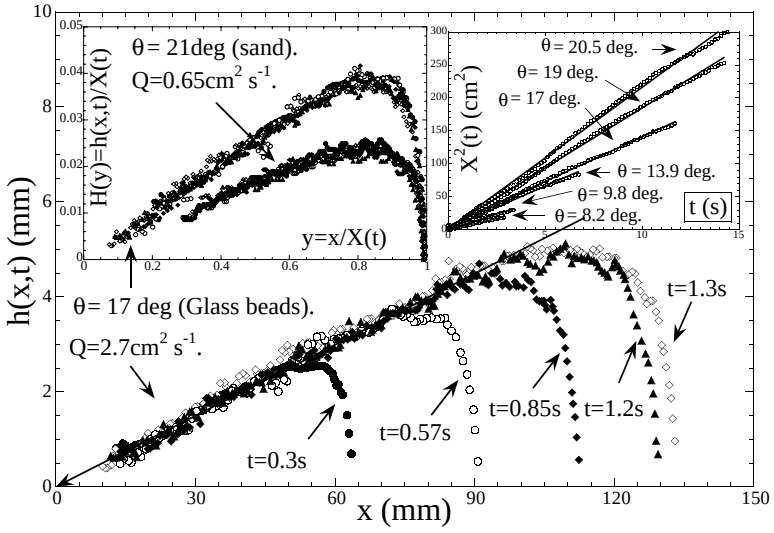

FIG. 2. Different sand fronts taken at different instants of time. Insets: Left, collapse of the profiles onto a single curve once the axes have been rescaled by the base length $X(t)$ for two values of the inclination angle. Right: Variation of $X^2(t)$ vs time for different inclination angles.

noted $h(x,t)$ $[0 \leqslant x \leqslant X(t), z=h(x,t)]$ are self-similar in time. More precisely with a reduced variable y and a reduced profile $H(y)$ one obtains the following scaling law:

$$x=yX(t), \quad 0 \leqslant y \leqslant 1, \quad h(x,t)=X(t)H(y). \tag{1}$$

The reduced profile $H(y)$ has features independent of the inclination θ, i.e., a strongly curved front part $(0.8<y\leqslant 1)$ corresponding to the deposition of the main part of the incoming flow and a quasilinear and very flat tail in its remaining part. If ϕ_0 denotes the angle between this tail and the OX axis, it is found that $T_0=\tan\phi_0$ depends upon θ according to

$$T_0(\theta) \simeq \lambda \tan(\theta_l-\theta), \tag{2}$$

where λ and θ_l are constants fixed by the granular materials. For sand $\lambda \simeq 0.4\pm0.05$, $\theta_l \simeq 27^\circ \pm 3^\circ$ and $\lambda \simeq 0.55\pm0.05$, $\theta_l \simeq 25^\circ \pm 3^\circ$ for glass beads, which shows that ϕ_0 decreases as θ increases and is always smaller than a maximal value of $\phi_0 \simeq 8^\circ$. In addition, it is stressed that such a behavior is observed only when the incoming flow is naturally trapped, its deceleration being due to friction following the Coulomb law, since the stopping length $L(\theta)$ measured along OX between injection and arrest varies as $L(\theta)=V_0^2/2ga(\theta)$ where $a(\theta)=\mu\cos\theta-\sin\theta$, μ being a dynamic friction coefficient, with a constant value ($\mu \simeq 0.46 \simeq \tan 25^\circ$ for sand). Arguments from energy balance are also given suggesting that $T_0(\theta) \sim a(\theta)$, which from Eq. (2) favors a value $\theta_l \simeq 25^\circ$ for sand. Finally, under various assumptions including scaling, a parametrization for the reduced profile $H_P(y)=T_0[y-\sinh(\nu y)/\sinh(\nu)]$ is proposed in order to reproduce the data when ν is properly adjusted.

III. DETERMINATION OF THE SANDPILE PROFILES

In this section we first show that the scaling, Eq. (1), appears as a consequence of the mass and energy conservation laws for a decelerating flow. To derive these relations, normalizing the density to one, we consider in the spirit of Ref. [6] $\partial_t h(x,t)=\Gamma(x,t)$ as the mass added per unit time to the sandpile at the point $(x,h(x,t))$. The complete deposition of the incoming flow on the sandpile then reads

$$\int_0^{X(t)} \Gamma(x,t+\delta)dx = Q, \tag{3}$$

where Q is the constant injected mass per unit time and δ the time delay needed by the rolling species to travel from $X(t)$ to x. We shall use this mass conservation relation in the instantaneous approximation $\delta=0$, which is justified in the following section, and systematically applied in the following.

A kinetic energy conservation law can also be derived according to the following assumptions. First, we recall that the incoming flow decelerates according to the friction Coulomb law and stops at the origin. Its velocity v_i just before impacting the sandpile at $x=X(t)$ is then known. At impact some dissipation may occur that we take into account by assuming that just after impact the mean velocity of the rolling species becomes $v_r=ev_i$ where e is a restitution coefficient, practically constant according to Ref. [9], for example, $e=0.4\pm0.05$. The kinetic energy then becomes $E=gQX(t)e^2a(\theta)$ and this energy is assumed to be lost by friction along the sandpile profile. In order to express the work of the friction forces one writes the Coulomb law with coefficient μ' (μ' refers to friction of sand on sand while μ refers to friction of sand against the flat plate) on some arc of the profile $h(u,t)$ with $x \leqslant u \leqslant X(t)$, the constant mass submitted to friction along this arc being $\Gamma(x,t)$ by definition. Summing all such arcs for $0 \leqslant x \leqslant X(t)$ gives the total friction work assumed to be equal to E. This kinetic energy conservation law then reads

$$\int_0^{X(t)} \Gamma(x,t)\{a'(\theta)[X(t)-x]+b(\theta)h(x,t)\}dx = QX(t)e^2a(\theta), \tag{4}$$

where $a'(\theta)=\mu'\cos\theta-\sin\theta$ and $b(\theta)=\mu'\sin\theta+\cos\theta$.

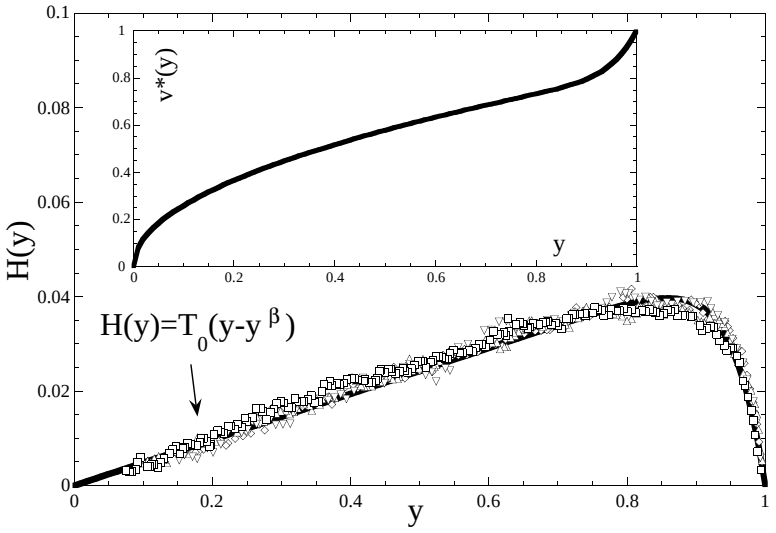

FIG. 3. A fit of the profile shape (different profiles have been collapsed onto the same curve here) using the expression in the text ($\beta=20$). Inset: Sketch of the dependence of the average velocity of the rolling grains along the sand front.

Now one can observe that the $X(t)$ dependence of Eq. (3,4) can be eliminated if $h(x,t)$ and $\Gamma(x,t)$ have appropriate scaling forms: $h(x,t)$ must obey Eq. (1) and $\Gamma(x,t)$ must be given by

$$\Gamma(x,t)=Q\gamma(y)/X(t), \tag{5}$$

where $\gamma(y)$ is some function of $y=x/X(t)$ alone. The conservation laws (3) and (4) then become time-independent constraints:

$$\int_0^1 \gamma(y)dy=1,$$

$$\int_0^1 \gamma(y)[a'(\theta)(1-y)+b(\theta)H(y)]dy=e^2a(\theta). \tag{6}$$

Our next task is to specify $X(t)$ and the reduced profile $H(y)$. One can easily obtain $X(t)$ from the global mass conservation if the mass of the rolling species is negligible (this is checked in the following section), since then the injected mass Qt is equal to the sandpile mass $\int_0^{X(t)}h(x,t)dx=X^2(t)I_H$ with $I_H=\int_0^1 H(y)dy$. This determines $X(t)$ in agreement with the experimental data:

$$X(t)=\sqrt{\alpha t},\quad \alpha=Q/I_H. \tag{7}$$

Having fixed $X(t)$, such that $X'(t)=\alpha/2X(t)$, one obtains from the scaling form, Eq. (1), $\partial_t h(x,t)=\alpha[H(y)-yH'(y)]/2X(t)$ which is equal to $\Gamma(x,t)$. (Here the prime symbol indicates total derivative in the function argument.) Using for $\Gamma(x,t)$ the expression given in Eq. (5), one obtains, since the $X(t)$ factor cancels, $H(y)-yH'(y)=2I_H\gamma(y)$. Integrating this relation with the boundary condition $H(y=1)=0$ gives

$$H(y)=2I_H y\int_y^1 u^{-2}\gamma(u)du. \tag{8}$$

In view of the central role devoted to $\gamma(y)$, we choose for it a physically realistic ansatz allowing simple integrations in Eqs. (6) and (8). Most of the deposition occurring in the region $y\simeq 1$, our choice is $\gamma(y)=(\beta+1)y^\beta$, where β is a free parameter and where the factor $(\beta+1)$ ensures the normalization appearing in Eq. (6). Then $H(y)$ given by Eq. (8) becomes $H(y)=2I_H[(\beta-1)/)(\beta+1)](y-y^\beta)$ and it can be checked on this form that the relation $I_H=\int_0^1 H(y)dy$ is identically fulfilled: at this stage $H(y)$ depends upon two free parameters I_H and β, the kinetic energy constraint remaining to be applied. These two parameters can be expressed in term of the more physical quantities T_0 and T_1 introduced in the first section and whose values are experimentally known (T_0 is small and $T_1\simeq 1$ and roughly independent of θ). The result of this substitution is

$$H(y)=T_0(y-y^\beta),\quad \beta=1+T_1/T_0\simeq 1/T_0,$$

$$I_H=T_1T_0/2(T_1+2T_0)\simeq T_0/2. \tag{9}$$

It thus appears that β has to be large (it varies from 10 to 32 according to the inclination angle), and this simplifies the remaining constraint in Eq. (6) which becomes independent of β in the large β limit. The energy conservation thus fixes T_0 according to

$$T_0=2e^2a(\theta)/b(\theta)\simeq 2e^2\tan(\theta_l-\theta), \tag{10}$$

where the last expression in Eq. (10) arises if $\mu'\simeq\mu=\tan\theta_l$. This is in agreement with the experimentally observed behavior given in Eq. (2) and gives the physical meaning of the parameter λ, $\lambda=2e^2$. For sand, a best fit of these data with $\theta_l=25°°$ gives $\lambda=0.37$, and for glass beads the best fit is $\theta_l=24°°$ with $\lambda=0.54$, giving for the restitution coefficient the realistic values $e=0.43$ and $e=0.52$, respectively. Figure 3 displays a fit to the experimentally observed profiles using experession (9) for $H(y)$. The agreement between the two shapes is remarkable.

IV. STUDY OF THE ROLLING SPECIES

In addition to the deposition term $\Gamma(x,t)$, the width $r(x,t)$ and the mean velocity $v_x(x,t)$ of the rolling grains on

top of the sandpile, which have been introduced in Sec. II, are the physical quantities used in the BCRE model to describe the flow. These quantities are not experimentally measured and our aim here is to show that they can be derived, as it is the case for the sandpile profile, in terms of $\gamma(y)$. As a by-product these results justify the simplifications used in the preceding section.

We first consider the quantity $m(x,t)=-v_x r(x,t)$ which is the rolling mass at abscissa x per unit time. In the instantaneous approximation $m(x,t)=Q-\int_x^{X(t)}\Gamma(u,t)du=\int_0^x\Gamma(u,t)du$. Inserting in the last integral Eq. (5) for $\Gamma(u,t)$ gives $m(x,t)=Q\int_0^y\gamma(u)du$ and for the total rolling mass Q_R one finds $Q_R=\int_0^{X(t)}m(x,t)dx=\int_0^{X(t)}\Gamma(x,t)[X(t)-x]dx$. Within the chosen ansatz for $\gamma(y)$ these relations become

$$m(x,t)=Qy^{\beta+1},\quad Q_R=QX(t)/(\beta+2), \tag{11}$$

which in particular indicate that the total rolling mass remains small compared to the sandpile mass.

We now turn to the determination of the mean velocity of the flow and we denote by $v(x,t)$ its absolute value. We have shown in the preceding section that its value v_r just after the impact point can be derived from energy considerations and is assumed to be given by $v(X(t),t)=v_r=eX(t)^{1/2}[2ga(\theta)]^{1/2}$. More generally, $v(x,t)$ can be obtained for any x by equating the kinetic energy variation and the friction work done on the sandpile between the points $X(t)$ and x. As in the preceding section, this work can be derived in terms of $\Gamma(x,t)$ and $h(x,t)$ which are now given. Using Eq. (10) for T_0 and some simplifications allowed in the large β regime, one finds the following scaling expression:

$$v(x,t)=v_r[y(2-y^{\beta+2})]^{1/2}=X(t)^{1/2}\omega(y),$$
$$\omega(y)=e[2ga(\theta)y(2-y^{\beta+2})]^{1/2}. \tag{12}$$

Assuming that this velocity is tangential to the sandpile profile and remembering that the tangent angle at abscissa x can be written as $\phi(y)$, its OX component reads $v_x(x,t)=-v(x,t)\cos\phi(y)$.

The width $r(x,t)$ of the rolling species is then given by the relation $r(x,t)=-m(x,t)/v_x(x,t)$ and we obtain the following scaling expression:

$$r(x,t)=X(t)^{-1/2}R(y),\quad R(y)=Qy^{\beta+1}/\omega(y)\cos\phi(y). \tag{13}$$

These relations indicate a rapid decrease of the width after the impact region and a slower one for the velocity. The functional shape of the velocity ($v^*=v/v_r$) along the profile is sketched in the inset of Fig. 3. This velocity starts out high and decreases to zero at the stopping point. The decrease of the velocity has two different regions, a region near the front with a fast decrease and a region towards the tail with a $\sqrt{y}$ dependence.

We conclude this section by checking the consistency of the instantaneous approximation that we have used to derive the scaling forms of various physical quantities $f(x,t)=X^n(t)F(y)$ with $-1\leqslant n\leqslant 1$. In this approximation $\delta=0$, where in reality $\delta=\int_x^{X(t)}du/v_x(u,t)$ is the time spent by the rolling species to travel from the point $(X(t),0)$ to the point $(x,h(x,t+\delta))$. The previous results show that $\delta=X^{1/2}(t)\Delta(y)$ where $\Delta(y)=\int_y^1 du/\omega(u)\cos(\phi(u))$ and thus $f(x,t+\delta)=f(x,t)[1+O(X^{-3/2}(t))]$. The instantaneous approximation thus gives correctly the leading behavior with time of the considered quantities.

V. CONCLUSION

In this phenomenological analysis, the BCRE formalism is used, but not in the usual way. We recall that in this model one considers a convective diffusion equation with diffusive constant D, which in our notations reads

$$(\partial_t-D\partial_x^2)r(x,t)=\partial_x m(x,t)-\Gamma(x,t). \tag{14}$$

This equation is used in conjunction with a functional relation of the form

$$\Gamma(x,t)=r(x,t)[A\partial_x h(x,t)+B\partial_x^2 h(x,t)] \tag{15}$$

to determine r,h, and Γ once the constants A,B, and an ansatz for v_x are given. In our case, Eq. (14) is implicitly satisfied as a convective equation since one can check that $\partial_x m(x,t)=\Gamma(x,t)$ and that its left-hand side member vanishes like $X^{-5/2}(t)$. On the other hand, the Eq. (15) does not hold as it appears that A and B are time-dependent: A vanishes like $X^{-1/2}(t)$ and the leading term is $B\simeq X^{1/2}(t)$. This reflects the experimental conditions, where the diffusion of the rolling species or shift from the repose angle is not essential for the dynamics of the sandpile profiles.

Before we conclude let us mention that Boutreux and Raphael [10] considered the stop flow problem, where a layer of mobile grains hits a wall, with a modified version of the BCRE model. Their version takes into account the inherent differences between thick and thin mobile layers. Their results show that for thick layers, a kink develops between the immobile grains and the mobile one. For thin layers, the height of the mobile part increases linearly with the distance from the wall. For intermediate thickness, the kink becomes blunt or slightly rounded. From these considerations, it appears that the case studied here, where the front is rounded, would fall in the category of intermediate thickness of the mobile grains. It may be interesting to solve their model for the particular geometry considered here so a comparison between their assumed form for the conversion term and the one constructed here can be made. Since their conversion term has a simple form, it would be interesting to test it more carefully.

In conclusion, we have given an explanation of the scaling law observed in this experiment, and we have proposed a phenomenological ansatz to describe the deposition mechanism. As a result it is possible to justify a simple analytic expression for the sandpile profile and to obtain a detailed description of its behavior under the variation of the inclination angle. This description involves one parameter β which is not fixed, contrarily to T_0, in terms of physical quantities,

except through the relation $\beta = 1 + T_1/T_0$. It may be thus possible to link the determination of T_1 to the stress tensor properties of the sandpile in its frontal part where it is submitted to the constraint of the incoming flow. This however needs a new formulation, such as the one proposed in Ref. [11], based on hydrodynamic equations for the flow coupled with an order parameter equation describing the transition between static and rolling species.

ACKNOWLEDGMENTS

We acknowledge fruitful discussions with Professor A. Wurger and Dr. F. Rioual.

[1] H.M. Jaeger, S.R. Nagel, and R.P. Behringer, Rev. Mod. Phys. **68**, 1259 (1996).

[2] S.B. Savage, in *Mechanics of Granular Materials*, edited by J.T. Jenkins and M. Satake (Elsevier, Amsterdam, 1983); A. Aradian, E. Raphael, and P.G. de Gennes, C. R. Phys. **3**, 187 (2002).

[3] A. Suzuki and T. Tanaka, Ind. Eng. Chem. Fundam. **10**, 84 (1971); E. Azanza, F. Chevoir, and P. Moucheront, J. Fluid Mech. **400**, 199 (1999); D.V. Khakhar *et al.*, *ibid.* **441**, 255 (2001).

[4] O. Pouliquen, Phys. Fluids **11**, 542 (1999).

[5] S.B. Savage and K. Hutter, J. Fluid Mech. **199**, 177 (1989); T. Boutreux, E. Raphael, and P.G. de Gennes, Phys. Rev. E **58**, 4692 (1998); S. Douady, B. Andreotti, and A. Daerr, Eur. Phys. J. B **11**, 131 (1999).

[6] J.P. Bouchaud, M.E. Cates, J. Ravi Prakash, and S.F. Edwards, J. Phys. I **4**, 1383 (1994).

[7] L. Mahadevan and Y. Pomeau, Europhys. Lett. **46**, 595 (1999).

[8] J-F. Boudet, S. Gauthier, Y. Amarouchene, and H. Kellay, Phys. Rev. E **67**, 010303(R) (2003).

[9] F. Rioual, A. Valance, and D. Bideau, Phys. Rev. E **62**, 2450 (2000).

[10] T. Boutreux and E. Raphael, Phys. Rev. E **58**, 7645 (1998).

[11] I.S. Aranson and L.S. Tsimring, Phys. Rev. E **64**, 020301 (2001).